



## Hydrolytic stability of nitrogenous-heteroaryltrifluoroborates under aqueous conditions at near neutral pH

Ying Li, Ali Asadi, David M. Perrin \*

Chemistry Department, University of British Columbia, 2036 Main Mall, Vancouver, British Columbia, Canada V6T-1Z1

### ARTICLE INFO

#### Article history:

Received 30 September 2008

Received in revised form 9 December 2008

Accepted 16 December 2008

Available online 27 December 2008

#### Keywords:

Heteroaryltrifluoroborates

$^{19}\text{F}$  NMR

Hydrolytic stability

PET imaging

### ABSTRACT

The hydrolytic stability of heteroaryltrifluoroborates under physiological conditions has been analyzed by  $^{19}\text{F}$  NMR spectroscopy and is found to be greatly enhanced by the presence of endocyclic ring nitrogens. Stability is further enhanced by the presence of exocyclic electron withdrawing substituents. As with aryltrifluoroborates, NMR analysis suggests that the hydrolysis proceeds via single rate-determining step reflecting loss of the first fluoride atom. The stability of these complexes is significant both in terms of metal catalyzed cross-coupling reactions as well as the potential for generating boronic acid based  $^{18}\text{F}$ -PET imaging agents.

© 2008 Elsevier B.V. All rights reserved.

### 1. Introduction

Potassium aryltrifluoroborates have aroused considerable attention recently due to their application in metal catalyzed coupling reactions [1–4]. This attention duly arises from the fact that aryltrifluoroborates are considerably more shelf-stable and resistant to oxidative side reactions than their corresponding boronic acids/esters from which they are prepared. In various studies, it has been shown that these non-coordinating anions are solubilized in water, which acts as an effective solvent for various transition metal catalysts. In addition, the common side reaction of protodeboronylation that occurs with boronic acids and esters can largely be suppressed by using aryltrifluoroborates as substrates. In the wake of many elegant synthetic investigations where aryltrifluoroborates have been used as stable substrates in catalytic C–C bond forming reactions, we suggested that arylboronic acids could be converted to  $^{18}\text{F}$ -labeled aryltrifluoroborates in a one-step aqueous labeling procedure to afford a suite of  $^{18}\text{F}$ -PET (positron emission tomography) imaging compounds [5].

For such application, one needs aryltrifluoroborates that are not just moderately stable to solvolytic defluoridation but extremely stable to solvolysis. Following that suggestion, it became important to address the chemical attributes that would govern the rate of aryltrifluoroborate solvolysis under aqueous conditions.

Indeed a Hammett analysis demonstrated that the rate constant for solvolytic defluoridation was found to correlate log-linearly with standard  $\sigma$ -values ( $\rho \sim -1$ ). This finding provided a chemical rationale as to why various aryltrifluoroborates are readily solvolyzed in water while others are considerably more stable [6], and guided the screening, identification, and synthesis of two chemically similar aryltrifluoroborates with extraordinary aqueous stability which was attributed to judicious placement of electron withdrawing substituents on the aryl ring [7,8]. One of these compositions was subsequently affixed to biotin and its *in vivo* stability was imaged by  $^{18}\text{F}$ -PET [7].

In light of these preliminary results with aryltrifluoroborates, here we address the potential of heteroaryltrifluoroborates for use in  $^{18}\text{F}$ -labeling and PET studies based on a hypothetical resistance to aqueous solvolysis, thus expanding the number of compositions that might ultimately prove useful for imaging. In so far as loss of the first fluoride is thought to precede transmetallation of the aryl moiety in Pd-catalyzed cross-coupling reactions, understanding the solvolytic stability of these valuable synthons also represents an important aspect in predicting their synthetic reactivity [1,9,10]. Because the manipulation of heterocyclic moieties via metal-catalyzed cross-coupling is essential for the ongoing design and synthesis of drugs, it is generally important to appreciate the stability of such heteroaryltrifluoroborates. Herein, we report the study of solvolysis of representative classes of nitrogenous heteroaryltrifluoroborates under buffered aqueous conditions at near-neutral pH by  $^{19}\text{F}$  NMR spectroscopy and thereby demonstrate that heteroaromatic ring systems greatly stabilize the trifluoroborates against aqueous solvolysis.

\* Corresponding author. Tel.: +1 604 822 0567; fax: +1 604 822 2847.

E-mail address: [dperrin@chem.ubc.ca](mailto:dperrin@chem.ubc.ca) (D.M. Perrin).

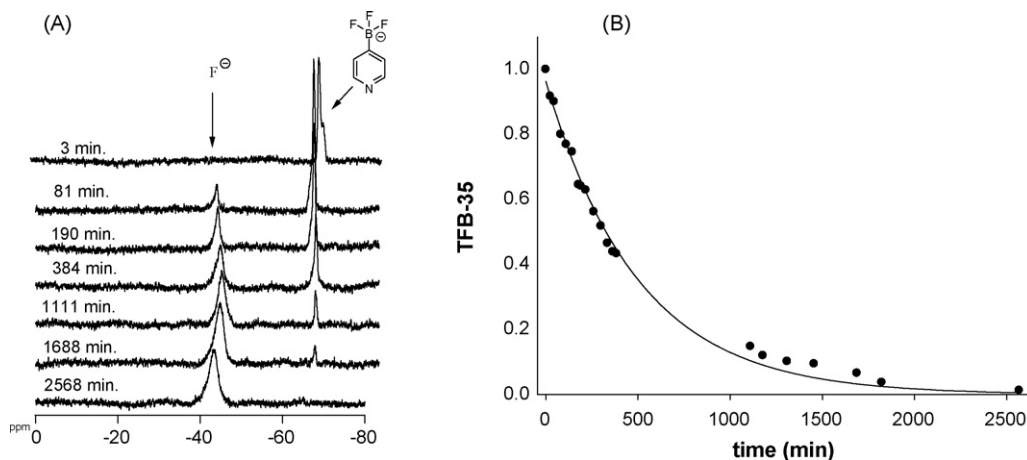


**Fig. 1.** Kinetic profile of *para*-pyridinyltrifluoroborate dissociation in aqueous solution. (A) *p*-Pyridinyl trifluoroborates (~65 ppm) dissociation monitored by  $^{19}\text{F}$  NMR; (B) plot of trifluoroborate fraction vs. time as measured by  $^{19}\text{F}$  NMR spectroscopy with signal of trifluoroacetic acid as the standard reference (0 ppm).

## 2. Results

The hydrolytic stabilities of several heteroaryltrifluoroborates were studied by  $^{19}\text{F}$  NMR spectroscopy. In general, it was found that at pH  $\sim 7$ , the half-lives of all the heteroaryltrifluoroborates were relatively long ( $t_{1/2} \geq 300$  min). From the  $^{19}\text{F}$  NMR spectroscopic assays, all cases showed a decrease in the aryltrifluoroborate signal ( $\sim 65$  ppm) and a concomitant increase in that of the free fluoride peak ( $\sim 42$  ppm) (Fig. 1). Interestingly, during the decomposition reaction, no obvious fluorinated intermediate appeared suggesting that any mono- and bis-fluorinated species rapidly hydrolyzed on the  $^{19}\text{F}$  NMR time scale. This observation allowed a facile kinetic analysis based on peak integration of both free fluoride and aryltrifluoroborate signals; the percentage of fluoride resident in the heteroaryltrifluoroborates at given time points was best fit to a typical first-order decay rate process for all decomposition assays. As such, these observations indicated that a single rate-determining step, which corresponded to the loss of the first fluoride atom, determined the overall rate of decomposition.

In an example of such kinetics studied by  $^{19}\text{F}$  NMR spectroscopy (Fig. 1), the *para*-pyridinyltrifluoroborate displayed a solvolytic half-life of 346 min ( $k_{\text{obs}} 0.0018 \pm 0.0008 \text{ min}^{-1}$ ). At higher pH (phosphate buffer), the rate constant for pyridinyltrifluoroborate solvolysis was only slightly elevated  $k_{\text{obs}}$  (pH 8.0) =  $0.0033 \pm 0.0002 \text{ min}^{-1}$ ;  $k_{\text{obs}}$  (pH 9.0) =  $0.0037 \pm 0.0001 \text{ min}^{-1}$ . Based on these results we extended this study of solvolysis at pH  $\sim 7$  to several readily prepared or commercially available heteroaryltrifluoroborates (Table 1). Briefly, the *para*-*N*-methylpyridiniumtrifluoroborate zwitterion, which is

prepared by  $\text{KHF}_2$  treatment of the corresponding boronate ester to give the *N*-methypyridinium analog, exhibits a 20-fold depression in the rate of solvolytic defluoridation. When exocyclic fluorine or chlorine atoms are introduced on the pyridine ring, the hydrolytic decomposition half-lives also increased significantly. The pyridazinyl trifluoroborates, which contain two ring nitrogens, exhibited even greater stability and some of these compounds showed extraordinary solvolytic stability even at higher temperatures.

## 3. Discussion

From these results, we conclude that the heteroaryltrifluoroborates exhibit high aqueous stability and are quite resistant to solvolytic defluoridation. By introducing additional exocyclic electron withdrawing groups on the heteroaromatic system, the stability of aryltrifluoroborates can be further increased. This additional stability derives from the fact that the inductive electron withdrawing effects of both the heteroatom ring nitrogens and exocyclic substituents reduces the available electron density that can be delocalized into the *p*-orbital on the boron atom, which is vacated upon solvolytic fluoride loss. Of the heteroaryltrifluoroborates investigated herein, the pyridazinyl trifluoroborates are found to be the most stable heteroaryltrifluoroborate salts and this study would suggest their use as  $^{18}\text{F}$ -PET imaging compounds for their high stability under the conditions which include higher temperatures.

Use of  $^{19}\text{F}$  NMR spectroscopy also permitted a convenient means of addressing the kinetics of aqueous defluoridation. In addition, we could not observe the appearance of any steady-state

**Table 1**  
Kinetic data for heteroaryltrifluoroborates (TFB).

Compound no.	Structure	Temperature	$k$ ( $\text{min}^{-1}$ )	$t_{1/2}$ (min)
TFB-35		$22 \pm 2$ °C	$(1.8 \pm 0.77) \times 10^{-3}$	$346 \pm 12$
		$22 \pm 2$ °C <sup>a</sup>	$(3.3 \pm 0.20) \times 10^{-3}$	$210 \pm 12$
		$22 \pm 2$ °C <sup>b</sup>	$(3.7 \pm 0.10) \times 10^{-3}$	$187 \pm 5$
TFB-AA-1		$22 \pm 2$ °C	$(8.00 \pm 0.21) \times 10^{-4}$	$866 \pm 22$

**Table 1** (Continued)

Compound no.	Structure	Temperature	$k$ (min <sup>-1</sup> )	$t_{1/2}$ (min)
TFB-YL2P008B		22 ± 2 °C 37 ± 2 °C 50 ± 2 °C	$(4.28 \pm 0.107) \times 10^{-5}$ $(1.07 \pm 0.025) \times 10^{-4}$ $(3.35 \pm 0.067) \times 10^{-4}$	16187 ± 404 6478 ± 150 2069 ± 41
TFB-66		22 ± 2 °C	$(1.90 \pm 0.068) \times 10^{-3}$	364 ± 13
TFB-95		22 ± 2 °C	$(0.6 \pm 0.016) \times 10^{-3}$	1155 ± 31
TFB-140		37 ± 2 °C 50 ± 2 °C	$(3.7 \pm 0.31) \times 10^{-5}$ $(1.2 \pm 0.046) \times 10^{-4}$	18698 ± 1563 5996 ± 240
TFB-yl-3-112		22 ± 2 °C 37 ± 2 °C 50 ± 2 °C	$(1.1 \pm 0.029) \times 10^{-4}$ $(5.2 \pm 0.20) \times 10^{-4}$ $(1.3 \pm 0.061) \times 10^{-3}$	6177 ± 158 1329 ± 51 527 ± 24

Note: the hydrolytic study without explanations was undertaken in 200 mM phosphate buffer at pH 6.87.

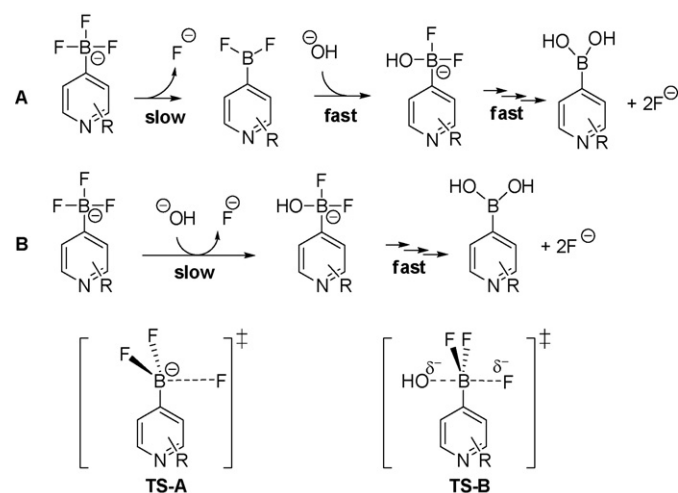
<sup>a</sup> The hydrolytic study was undertaken in 200 mM phosphate buffer at pH 8.01.

<sup>b</sup> The hydrolytic study was undertaken in 200 mM phosphate buffer at pH 9.00.

intermediate on the NMR time scale which leads us to conclude that while the mechanism of heteroaryltrifluoroborate solvolysis must involve at least three sequential steps of fluoride loss, only one rate-limiting step is sufficient to describe the entire defluorination reaction, as shown in Scheme 1. In our hands, the resulting heteroarylboronic acid products often precipitated due to low solubility and/or potential aggregation. Since no intermediates were observed by NMR spectroscopy for any of the compounds

studied in this work, the second and third hydroxide-fluoride exchange processes must be fast such that no difluoro- and monofluoroborate/borate intermediates accumulate.

Based on these observations, it is likely that rate limiting B-F bond dissociation proceeds via an S<sub>N</sub>1-like mechanism (Mechanism A, Scheme 1), that is independent of the nucleophile concentration, which would be either water or hydroxide ion. Corroborating this assertion is the finding that, at least for the



**Scheme 1.** Hypothetical mechanism for the hydrolysis of heteroaryltrifluoroborates. TS-x is the transition state for the slow step of either mechanism.

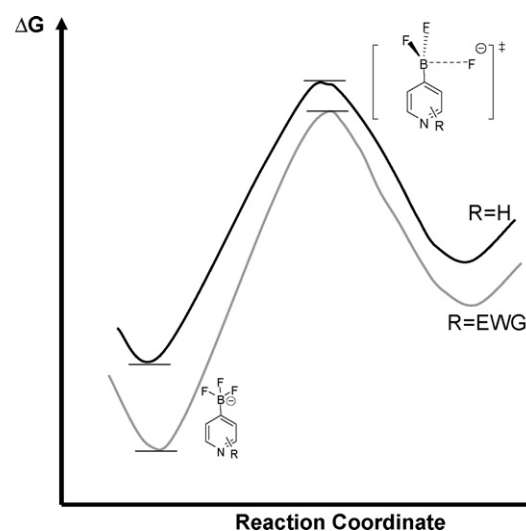


**Fig. 2.** Hypothetical energy diagram of hydroxide-fluoride exchange for step 1 of mechanism A. The electron withdrawing groups (EWG) can largely stabilize the starting materials while the stabilizing effect is much weaker for transition states.

*para*-pyridinyltrifluoroborate, the value of  $\log(k_{obs})$  for solvolysis is essentially pH independent rather than being linearly correlated with pH as would be expected for an  $S_N2$ -like mechanism (Mechanism B, Scheme 1), which would involve hydroxide ion as a nucleophile attacking boron in a pentacoordinate transition state.

In terms of the overall reaction coordinate, one must consider the relative stabilities of both the ground state and transition state. As noted, the heteroaryltrifluoroborates with stronger electron withdrawing groups have higher stability against hydrolysis. This might be interpreted by considering the energy of the ground state of starting materials as well as that of the transition states. The electron withdrawing groups discussed here exert strong inductive effects which serve to decrease the *p*-electron density available for conjugation into an empty *p*-orbital on an  $sp^2$ -hybridized boron atom, which in turn renders the boron–fluoride bonds much more robust. In addition, the energy gap between the ground state and transition state is also increased by the presence of electron withdrawing groups as it is possible that the presence of EWG stabilizes the trifluoroborate anion (Fig. 2).

#### 4. Conclusion

Herein we have addressed the hydrolytic stability of several heteroaryltrifluoroborates by  $^{19}\text{F}$  NMR spectroscopy. The heteroaryltrifluoroborates exhibit a very high degree of stability against hydrolytic decomposition. For the development of new PET imaging compounds, this study identifies new heteroaryltrifluoroborates that exhibit much longer half-lives for solvolytic decomposition than that of the nuclear decay of  $^{18}\text{F}$ -fluorine itself. For metal catalyzed coupling reactions, it has also been hypothesized that the active substrates for cross-coupling are base-coordinated dihydroxyboronate salts rather than trifluoroborates. Consistent with this hypothesis is the observation that aryltrifluoroborates with strong electron withdrawing groups are more recalcitrant to transition metal catalyzed activation. Because defluorination has been invoked as a necessary step to regenerate the arylboronate *in situ*, our findings suggest that the extraordinary stability of these aryltrifluoroborates would render them refractory for use under standard cross-coupling conditions. Nevertheless, that same recalcitrance suggests that the same heteroaryltrifluoroborates should be outstanding candidate compositions for *in vivo* PET imaging.

#### 5. Experimental

The heteroaryltrifluoroborates were prepared via fluoridation of corresponding heteroarylboronic acids or heteroarylboronate esters. Heteroaryltrifluoroborates for kinetic study were then purified on a 0.5 cm silica column using 5%  $\text{NH}_4\text{OH}$  in ethanol as the eluent.

For  $^{19}\text{F}$  NMR spectroscopic analysis, the ratio of aryltrifluoroborate signal to the total  $^{19}\text{F}$  signal was plotted against time in Eq. (1):

$$R_t = R_0 e^{-k_{obs}t} \quad (1)$$

where  $R_t$  and  $R_0$  are the ratios of values corresponding to heteroaryltrifluoroborate integration and total  $^{19}\text{F}$  integration at time  $t$  and 0 min, respectively. The half-life of each compound was calculated by dividing natural log of 2 by the observed rate constant  $k_{obs}$  ( $\ln 2/k_{obs}$ ). Since the solvolysis of some heteroaryltrifluoroborates proceeded so slowly at room temperature, higher temperatures (37 and 50 °C) were employed.

#### 5.1. Synthetic procedures

Arylboronic acid precursors to TFB-35, TFB-66, TFB-95, TFB-140 were obtained from Sigma–Aldrich or Alfa Aesar. Deuterated solvents were purchased from Cambridge Isotope Laboratories. Analytical thin layer chromatography was run on Silica Gel 60  $\text{F}_{254}$ . Glass TLC plates from EMD Chemicals and silica F60 from Silicycle were used for chromatography. Melting points were not corrected and are reported using two different melting-temperature apparatuses for consistency of the indicated values. Differences from literature reports may be due to the presence of trace impurities or errors in prior reports.

##### 5.1.1. Triaminoguanidine monohydrochloride (1) [11]

Hydrazine monohydrate 3.41 g (68.2 mmol) was added to a suspension of 1.91 g (20.0 mmol) of guanidine hydrochloride in 10 mL of 1,4-dioxane at room temperature. The mixture was then stirred under reflux until ammonia was no longer released. The reaction mixture was cooled to room temperature, filtered, washed with 1,4-dioxane and dried. 2.49 g (88%) of white powder was obtained, mp 215–216 °C (Lit. 230 °C).  $^{13}\text{C}$  NMR ( $\text{D}_2\text{O}$ , 75.5 MHz, room temperature):  $\delta$  (ppm) 159.7. ESI:  $[\text{M}-\text{Cl}]^+$ : 104.9 (100%).

##### 5.1.2. 3,6-Bis(3,5-dimethylpyrazol-1-yl)-1,2-dihydro-1,2,4,5-tetrazine (2) [11]

14.1 g (0.100 mol) of triaminoguanidine monohydrochloride (1) in 100 mL of water was added dropwise to 20.4 g (0.2 mol) of 2,4-pentanedione at room temperature. The mixture was then heated at 70 °C overnight after stirring at room temperature for 0.5 h. The orange precipitate was then filtered, washed with water, and dried after the mixture was cooled to room temperature. 10.8 g (80%) of pure 2 was obtained, mp 130–131 °C (Lit. 150 °C).  $^1\text{H}$  NMR ( $d_6$ -DMSO, 300 MHz, room temperature):  $\delta$  (ppm) 2.15 (s, 2 $\text{CH}_3$ ), 2.38 (s, 2 $\text{CH}_3$ ), 6.12 (s, 2CH), 8.82 (s, 2NH);  $^{13}\text{C}$  NMR ( $d_6$ -DMSO, 75.5 MHz, room temperature):  $\delta$  (ppm) 13.53, 13.84, 110.03, 142.29, 145.88, 149.99. ESI:  $[\text{M}+\text{H}]^+$ , 273.2 (100%), 273.4 (15%).

##### 5.1.3. 3,6-Bis(3,5-dimethylpyrazol-1-yl)-1,2,4,5-tetrazine (3) [11]

$\text{NO}/\text{NO}_2$  was produced by adding 78 mL of 50% sulfuric acid dropwise to 100 mL 0.6 N sodium nitrite; the resulting gas was bubbled into 40 mL of DMF containing 2.26 g (8.3 mmol) of 2 at room temperature over the period of 4 h. Then 100 mL of ice water was added to the DMF solution resulting in a purple precipitate. The reaction mixture was filtered, washed with cold water and dried. 1.61 g (72%) of 3 was obtained, mp 216–218 °C (Lit. 223–224 °C).  $^1\text{H}$  NMR ( $d_6$ -DMSO, 300 MHz, room temperature):  $\delta$  (ppm) 2.27 (s, 2 $\text{CH}_3$ ), 2.58 (s, 2 $\text{CH}_3$ ), 6.35 (s, 2CH);  $^{13}\text{C}$  NMR ( $d_6$ -DMSO, 75.5 MHz, room temperature): 14.05, 14.25, 111.58, 143.70, 153.18, 159.37. ESI:  $[\text{M}+\text{Na}]^+$ : 293.2 (100%), 294.2 (15%).

##### 5.1.4. 3,6-Dihydrazino-1,2,4,5-tetrazine (4) [12]

1.3 g (26 mmol) of hydrazine monohydrate was added slowly to a slurry of 3 (3.2 g, 12 mmol) in 30 mL of acetonitrile. The resulting dark red solution was then heated to reflux for 1.5 h. After cooling to room temperature, the mixture was filtered and the filter cake was washed with acetonitrile to afford 1.22 g (73%) of dark red product, mp 137–138 °C.  $^{13}\text{C}$  NMR ( $d_6$ -DMSO, 75.5 MHz, room temperature): 163.97. ESI:  $[\text{M}+\text{H}]^+$ : 143.1 (100%).

##### 5.1.5. 3,6-Dichloro-1,2,4,5-tetrazine (5) [13]

To the slurry of 3,6-di(hydrazino)-1,2,4,5-tetrazine (4) (1.28 g, 9 mmol) in 35 mL of acetonitrile at 0 °C was added dropwise 25 mL of acetonitrile containing 4.08 g (18 mmol) of trichloroisocyanuric acid for a period of 30 min. The reaction mixture was then allowed to warm up to room temperature over a period of 20 min. After filtration, the filtrate was concentrated under vacuum to give crude

5. A quantity of 0.63 g (46%) in pure crystalline form of orange color was obtained via sublimation.  $^{13}\text{C}$  NMR ( $\text{CDCl}_3$ , 75.5 MHz, room temperature): 168.24. ESI: $[\text{M}+\text{H}]^+$ : 149.8 (100%), 151.8 (67%).

#### 5.1.6. 2-(1-Hexyn-1-yl)-4,4,5,5-tetramethyl-1,3,2-dioxaborolane (**6**) [14]

Two grams (24 mmol) of *n*-hexyne in 24 mL of dry diethyl ether was cooled to  $-78^\circ\text{C}$  and then 15.2 mL (24.32 mmol) of 1.6 M *n*-butyl lithium was added. The resulting slurry was stirred for 0.5 h at  $-78^\circ\text{C}$  and then 4.58 g (24.6 mmol) of 2-isopropoxy-4,4,5,5-tetramethyl-1,3,2-dioxaborolane in 24 mL of dry diethyl ether was added quickly to the mixture via syringe and the mixture was stirred at the same temperature for another 2 h. The reaction mixture was then warmed to room temperature and stirred at room temperature for an additional hour, whereupon the mixture was cooled to  $-78^\circ\text{C}$  and 5.4 mL of 4.5 M hydrochloric acid in dry diethyl ether was added. The slurry was then stirred for an addition 20 min and then warmed to room temperature. After filtration, solvent was removed under vacuum and 1.86 g (37%) of colorless product **6** was obtained via distillation at  $75\text{--}80^\circ\text{C}$  over 1–1.5 mmHg.  $^1\text{H}$  NMR ( $\text{CDCl}_3$ , 300 MHz, room temperature):  $\delta$  (ppm) 0.86 (t,  $J = 7.2$  Hz,  $1\text{CH}_3$ ), 1.23 (s,  $4\text{CH}_3$ ), 1.28–1.50 (m,  $2\text{CH}_2$ ), 2.22 (t,  $J = 7.0$  Hz,  $\text{CH}_2$ );  $^{13}\text{C}$  NMR ( $\text{CDCl}_3$ , 75.5 MHz, room temperature):  $\delta$  (ppm) 13.61, 19.30, 21.99, 24.75, 30.23, 82.51, 83.16, 84.08.  $^{11}\text{B}$  NMR ( $\text{CDCl}_3$ , 128.4 MHz, room temperature):  $\delta$  (ppm) 21.47 (d,  $J = 95$  Hz).

#### 5.1.7. 4-Butyl-3,6-dichloro-5-(4,4,5,5-tetramethyl-1,3,2-dioxaborolan-2-yl)pyridazine (**YL2P008B**) [13]

0.32 g (1.9 mmol) of **6** and 0.152 g (1.28 mmol) of tetrazine **5** was mixed in 7 mL of xylenes. The mixture was then heated to reflux under nitrogen flow for a period of 24 h. Solvent was removed under vacuum. The residue was eluted purified by standard flash column chromatography using ethyl acetate in hexanes (1:30, v/v). A lightly red colored oil was obtained: 69 mg (14%).  $^1\text{H}$  NMR ( $\text{CDCl}_3$ , 300 MHz, room temperature):  $\delta$  (ppm) 0.95 (t,  $J = 7.2$  Hz,  $\text{CH}_3$ ), 1.40 (s,  $4\text{CH}_3$ ), 1.43 (m,  $\text{CH}_2$ ), 1.55 (m,  $\text{CH}_2$ ), 2.69 (t,  $J = 8.1$  Hz,  $\text{CH}_2$ );  $^{13}\text{C}$  NMR ( $\text{CDCl}_3$ , 75.5 MHz, room temperature):  $\delta$  (ppm) 13.83, 23.09, 24.85, 31.63, 33.59, 85.99, 147.88, 157.65, 147.88;  $^{11}\text{B}$  NMR ( $\text{CDCl}_3$ , 128.4 MHz, room temperature):  $\delta$  (ppm) 29.78; HRMS  $[\text{M}+\text{H}]^+$ : calcd. for  $\text{C}_{14}\text{H}_{22}\text{BCl}_2\text{N}_2\text{O}_2$ : 331.1151, found: 331.1146.

#### 5.1.8. *N*-Methyl-4-(4,4,5,5-tetramethyl-1,3,2-dioxaborolan-2-yl)pyridinium iodide (**YL-3-112**) [15]

Briefly, 0.5 g (4 mmol) of 4-pyridinylboronic acid and 0.4 g (4 mmol) of 2,2-dimethyl-1,3-propanediol were dissolved in 1,4-dioxane and a few chips of 4 Å molecular sieves were added to the solution. The mixture was heated to reflux for 18 h. The reaction was then cooled to room temperature and filtered to remove the molecular sieves. The solution was condensed under vacuum and the residue was dried over high vacuum to give 0.85 g (quantitatively) of a white solid which that was used without further purification. The white solid representing the dimethyl-propanediolboronate was dissolved in 25 mL of acetonitrile and 2.4 mL (40.2 mmol) of methyl iodide was added. The mixture was then refluxed overnight. Solvent was removed under vacuum after cooling the reaction slurry to room temperature. To the yellowish residue, 30 mL of 1:1 (v/v) water/acetone was added and the slurry was stirred at room temperature for 1 d. The mixture was then clarified by filtration and the filtrate was concentrated. The product was precipitated from methanol/diethyl ether to give 1.02 g (overall 74%) of yellowish solid.  $^1\text{H}$  NMR ( $d_6$ -DMSO, 400 MHz, room temperature):  $\delta$  (ppm) 4.2 (s,  $\text{CH}_3$ ), 7.54 (d,  $J = 6.0$  Hz, Ar-H), 8.55 (d,  $J = 6.0$  Hz, Ar-H);  $^{13}\text{C}$  NMR ( $d_6$ -DMSO, 100.6 MHz, room temperature):  $\delta$  (ppm) 48.82, 50.08, 132.14,

144.32;  $^{11}\text{B}$  NMR ( $d_6$ -DMSO, 128.4 MHz, room temperature):  $\delta$  (ppm) 3.12.

#### 5.1.9. 2,6-dichloropyridine-4-boronic acid (**AA-1**):

2,6-Dichloro-4-iodo-pyridine was prepared according to literature protocol [16] and then lithiated with *n*-butyl lithium followed by quenching with trimethoxyborate. Briefly, 2,6-dichloro-4-iodo-pyridine (1.4 g, 10 mmol) at  $-75^\circ\text{C}$  was added to a solution of butyllithium (15 mmol) in dry ether (30 mL) and hexanes (8 mL). After 30 min at  $-75^\circ\text{C}$ , the mixture was treated with trimethoxyborate (1.25 mL, 11 mmol) and was allowed to stir for 1 h. The temperature was allowed to rise slowly over a period of 2 h to room temperature at which point first pinacol (1.6 g, 13 mmol, 1.1 equiv.) and then 10 min later AcOH (0.6 mL, 10 mmol) was added. The resulting mixture was filtered through celite, which was then washed with ether, and the combined filtrates were evaporated under reduced pressure. The desired product was crystallized from cyclohexane (1.4 g, 74%).  $^1\text{H}$  NMR ( $\text{CDCl}_3$ , 300 MHz, room temperature):  $\delta$  (ppm) 1.34 (s, 12 H), 8.06 (s, 2H).  $^{13}\text{C}$  NMR ( $\text{CDCl}_3$ , 75.5 MHz, room temperature):  $\delta$  (ppm) 24.8, 84.4, 111.9, 128, 149.

#### 5.2. Preparation of heteroaryltrifluoroborates

General protocol: boronic acid/ester, potassium hydrogen difluoride ( $\text{KHF}_2$ ) and acetic acid were mixed in either aqueous acetonitrile, methanol, or DMSO (depending on the solubility of the compounds) to make a final cocktail containing 5 mM of boronic acid/ester and 200 mM of  $\text{KHF}_2$  and 1.8 M acetic acid. The reaction mixture was stored at room temperature and the reaction could be monitored by TLC using 10% (v/v) ammonium hydroxide in ethanol as the mobile phase. Generally, the reactions were left for 2 days to ensure 100% conversion to the heteroaryltrifluoroborate in solution. Just prior to use, the heteroaryltrifluoroborates were purified either by column with 5% (v/v) ammonium hydroxide in ethanol or by extraction of the organic portion (pinacol, protideboronylated material, or other organic contaminants) with suitable organic solvents after removal of the reaction solvent. Products corresponding to unknown heteroaryltrifluoroborates were characterized by high-resolution mass spectrometry and the solvolytic defluorination was monitored by  $^{19}\text{F}$  NMR spectroscopy. Products previously obtained in this manner from literature preparations were used without further characterization.

**TFB-35** HRMS (ESI)  $[\text{M}]^-$ : Calculated for  $\text{C}_5\text{H}_4\text{BNF}_3^-$ : 146.0389, Found. 146.0385.

**TFB-95** HRMS (ESI)  $[\text{M}]^-$ : Calculated for  $\text{C}_5\text{H}_2\text{BNF}_5^-$ , 182.0200, Found. 182.0196.

**TFB-YL3-112** HRMS (ESI)  $[\text{M}+\text{K}]^+$ : Calculated for  $\text{C}_6\text{H}_7\text{BNF}_3\text{K}^+$ , 200.0261, Found. 200.0257.

**TFB-66** HRMS (ESI)  $[\text{M}]^-$ : Calculated for  $\text{C}_5\text{H}_3\text{BNF}_4^-$ , 164.0295, Found. 164.0292.

#### Acknowledgements

D.M.P. was the recipient of a Michael Smith Career Scholar Award. The authors thank Dr. Curtis Harwig and Dr. Richard Ting for useful advice. This work was supported by Canadian Institutes for Health Research.

#### References

- [1] G.A. Molander, B. Biolatto, *Org. Lett.* 4 (2002) 1867–1870.
- [2] G.A. Molander, B. Biolatto, *J. Org. Chem.* 68 (2003) 4302–4314.
- [3] R. Cella, R.L.O.R. Cunha, A.E.S. Reis, D.C. Pimenta, C.F. Klitzke, H.A. Stefani, *J. Org. Chem.* 71 (2006) 244–250.
- [4] T.D. Quach, R.A. Batey, *Org. Lett.* 5 (2003) 1381–1384.

- [5] R. Ting, M.J. Adam, T.J. Ruth, D.M. Perrin, *J. Am. Chem. Soc.* 127 (2005) 13094–13095.
- [6] R. Ting, C. Harwig, J. Lo, Y. Li, M.J. Adam, T.J. Ruth, D.M. Perrin, *J. Org. Chem.* 73 (2008) 4662–6670.
- [7] R. Ting, C. Harwig, U.a.d. Keller, S. McCormick, P. Austin, C.M. Overall, M.J. Adam, T.J. Ruth, D.M. Perrin, *J. Am. Chem. Soc.* 130 (2008) 12045–12055.
- [8] R. Ting, J. Lo, M.J. Adam, T.J. Ruth, D.M. Perrin, *J. Fluorine Chem.* 129 (2008) 349–358.
- [9] T.E. Barder, S.L. Buchwald, *Org. Lett.* 6 (2004) 2649–2652.
- [10] G.A. Molander, T. Fumagalli, *J. Org. Chem.* 71 (2006) 5743–5747.
- [11] M.D. Coburn, G.A. Buntain, B.W. Harris, M.A. Hiskey, K.Y. Lee, D.G. Ott, *J. Heterocycl. Chem.* 28 (1991) 2049–2050.
- [12] D.E. Chavez, M.A. Hiskey, *J. Heterocycl. Chem.* 35 (1998) 1329–1332.
- [13] M.D. Helm, A. Plant, J.P.A. Harrity, *Org. Biomol. Chem.* 4 (2006) 4278–4280.
- [14] H. Abu Ali, A. El Aziz Al Quntar, I. Goldberg, M. Srebnik, *Organometallics* 21 (2002) 4533–4539.
- [15] T. Maki, K. Ishihara, H. Yamamoto, *Org. Lett.* 7 (2005) 5043–5046.
- [16] E. Marzi, A. Bigi, M. Schlosser, *Eur. J. Org. Chem.* 2001 (2001) 1371–1376.